

Synthesis, Structure, and Ligand-Centered Catalytic Properties of M^{II} Coordination Polymers ($M = Zn^{II}, Cd^{II}, Hg^{II}$) with Open Pyridyl *N*-Oxide Sites

Jun-Yan Cheng, Feng-Wen Ding, Peng Wang, Chao-Wei Zhao, and Yu-Bin Dong^{*[a]}

Four M^{II} ($M = Zn^{II}, Cd^{II}, Hg^{II}$) coordination polymers were designed and synthesized based on two pyridine *N*-oxide bridging ligands: 3,5-bis(4-pyridyl)pyridine *N*-oxide and 2,6-bis(3-pyridyl)pyridine *N*-oxide. The resulting polymers all feature a one-dimensional chain motif and contain free pyridyl moieties.

More importantly, they exhibit interesting ligand-centered (pyridyl *N*-oxide) catalytic behavior, and can be used as highly heterogeneous catalysts to promote the Knoevenagel condensation reaction under ambient conditions.

Introduction

Coordination polymers (CPs), as a new class of organic–inorganic hybrid materials, have received intense attention owing to their potential applications in gas adsorption and purification,^[1] luminescence,^[2] drug delivery, and so on.^[3] On the other hand, CPs provide a practical platform to fabricate new types of heterogeneous catalytic materials.^[4] In principle, CPs can act as solid catalysts, based on either catalytically active metal centers (metal-centered CPs catalysts)^[5] or functional organic groups attached to the ligands (ligand-centered CPs catalyst).^[6] For example, metal-centered CP catalysts, especially those with open metal sites, can be considered as Lewis acid type catalytic species to promote reactions such as carbon–carbon and carbon–heteroatom bond formation, C–H bond activation, and hydrogenation. On the other hand, ligand-centered CP catalysts usually behave as Lewis base type catalysts owing to the Lewis basicity of the organic functional groups in the ligand, such as pyridine, amide, and amine moieties. Such CPs can be used to facilitate ester polymerization, Knoevenagel condensation, the Michael reaction, and so on. Compared with metal-centered CPs catalysts, the design and synthesis of the ligand-centered CP counterparts are more challenging because the embedded catalytically active organic groups might also coordinate to the metal nodes during the self-assembly process as a result of their Lewis base nature.

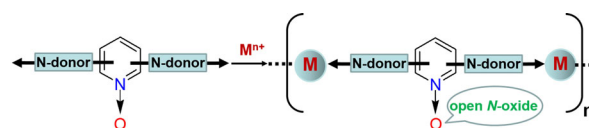
We have been studying CPs with different topological structural motifs composed of metal ions and functional organic linkers.^[7] In our previous study, bridging *N*-oxides were designed and used as ligands to construct CPs with adsorption/separation or fluorescence properties.^[8] *N*-Oxides, as typical homogeneous catalysts, are widely used in the catalysis of nucleophilic organic reactions in both metal-free or -mediated forms owing to their pronounced nucleophilic character.^[9] Despite fruitful advancements in academia, similar to many homogeneous catalytic species, they cannot be more extensively applied because of inherent difficulties in separation of the catalysts from the reaction systems.

Compared with homogeneous catalytic systems, heterogeneous catalysts are more long-lived for recyclable use than their homogeneous counterparts. To solve this problem, the embedding of the catalytic active *N*-oxides species through covalent-bonding interactions into solid CPs can be performed. Based on this approach, *N*-oxide species can become reusable and eco-friendly catalysts for practical application. For example, the pyridine *N*-oxide unit could be introduced into divergent organic ligands that contain different types of coordinating donors. In addition, coordinating donors, other than *N*-oxides, can bind relatively “soft” metal ions in CPs (Scheme 1). The obtained CPs with free *N*-oxides are expected to be effective heterogeneous solid catalysts for promoting organic reactions. To date, the catalytic activity of CPs with free *N*-oxides as Lewis base sites has remained unexplored.

Herein, we report two new, rigid, bent ligands, namely, 3,5-bis(4-pyridyl)pyridine *N*-oxide (**L1**) and 2,6-bis(3-pyridyl)pyridine

[a] J.-Y. Cheng, F.-W. Ding, Dr. P. Wang, C.-W. Zhao, Prof. Dr. Y.-B. Dong
College of Chemistry, Chemical Engineering and Materials Science
Collaborative Innovation Center of Functionalized Probes
for Chemical Imaging in Universities of Shandong
Key Laboratory of Molecular and Nano Probes, Ministry of Education
Shandong Normal University, Jinan 250014 (P. R. China)
E-mail: yubindong@sdu.edu.cn

Supporting information for this article can be found under <http://dx.doi.org/10.1002/cplu.201600009>. It contains ORTEP figures, selected bond lengths and angles for 1–5, and GC-MS and GC analysis data for catalytic reactions based on 1–4.



Scheme 1. Design of the *N*-oxide-containing organic ligand and corresponding CPs with open *N*-oxide sites.

This article is part of a Special Issue on “Coordination Polymers/MOFs”. A link to the issue will appear here once it is compiled.

N-oxide (**L2**), with both pyridyl and pyridyl *N*-oxide groups. As shown in Scheme 2, ligands **L1** and **L2** were prepared by Suzuki–Miyaura cross-coupling reactions between bromine-substituted pyridine *N*-oxide and the corresponding pyridine boronic acids in good yields. Ligands **L1** and **L2** have the following features: 1) both contain pyridyl and *N*-oxide donors with different coordinating natures; and 2) they are generally expected to link relatively soft metal ions, such as zinc(II) and cadmium(II), to CPs with a free *N*-oxide moiety, as potential

Lewis base type catalysts for specific organic reactions. Furthermore, four CPs based on these ligands have been synthesized (Scheme 2). They all display a 1D chain motif with an open pyridine *N*-oxide site. Notably, compounds **1–4**, with free pyridine *N*-oxide moieties, are the first highly active heterogeneous CP catalysts for Knoevenagel condensation.

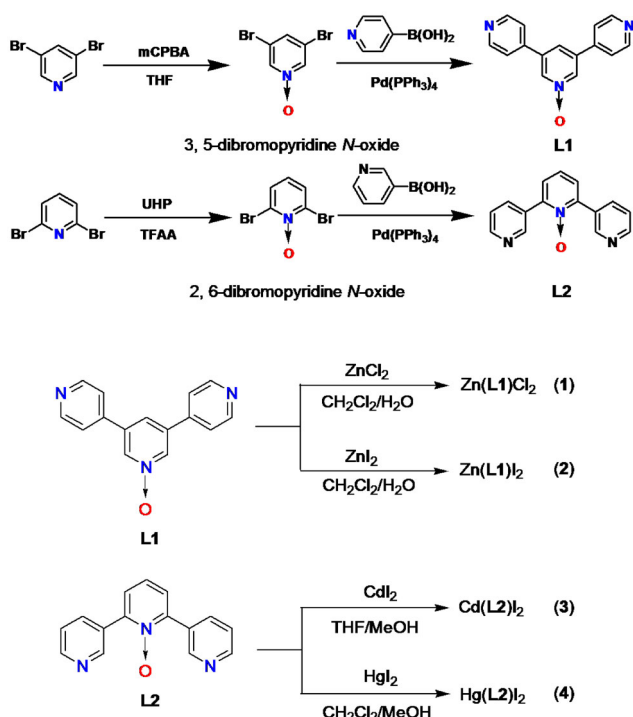
Results and Discussion

Structural analysis

M^{II} CPs based on **L1**

The crystallization of **L1** with ZnCl₂ and ZnI₂ (metal-to-ligand ratio 1:1) in a mixture of CH₂Cl₂/CH₃OH at room temperature afforded **1** and **2** as colorless crystals, respectively. Single-crystal X-ray analysis revealed that **1** (Zn(L1)Cl₂) and **2** (Zn(L1)I₂) were isostructural; thus only the structure of **1** is described in detail herein (Table 1).

Compound **1** crystallizes in the monoclinic space group *P21/c*. There is only one crystallographic zinc(II) center in **1**. As shown in Figure 1, the zinc(II) node lies in a slightly distorted tetrahedral coordination sphere that consists of two terminal N_{pyridyl} donors on **L1** and two Cl[−] counterions. The corresponding Cl₂–Zn1–Cl1 and N2–Zn1–N3 angles are 128.2 and 109.53°, respectively. The Zn–N bond lengths are 2.044(3) and 2.045(3) Å, respectively, and they all are within the range of reported Zn^{II}–N bond lengths.^[10] Notably, pyridyl-*N*-oxides groups in **1** are free and uncoordinated to the zinc(II) centers. As indicated in Figure 1, ligand **L1** acts as a bidentate ligand to bind zinc(II) cations through terminal pyridyl nitrogen atoms into 1D helical chains that extend along the crystallographic *b* axis. These one-handed 1D chains are further connected to each other through interchain hydrogen-bonding interactions into a chiral 2D wave-shaped layer. The hydrogen-bonding system is composed of the oxygen atom of pyridyl *N*-oxide and a hydrogen atom of pyridyl *N*-oxide on a neighboring chain (Figure 1). The *P* and *M* layers alternatively arrange along



Scheme 2. Synthesis of **L1**, **L2**, and compounds **1–4**. mCPBA = 3-chloroperbenzoic acid, UHP = urea hydrogen peroxide, TFAA = trifluoroacetic acid anhydride.

Table 1. Crystal data and structural refinement parameters for **1–5**.

	1	2	3	4	5
formula	C ₁₅ H ₁₁ Cl ₂ N ₃ OZn	C ₁₅ H ₁₁ I ₂ N ₃ OZn	C ₁₅ H ₁₁ I ₂ N ₃ OCd	C ₁₅ H ₁₁ I ₂ N ₃ OHg	C ₆₀ H ₄₄ I ₁₂ N ₁₂ O ₄ Cd ₆
<i>M_r</i>	385.56	568.44	615.48	703.66	3194.33
crystal system	monoclinic	monoclinic	monoclinic	monoclinic	tetragonal
<i>a</i> [Å]	7.3299(19)	7.2321(4)	9.7914(15)	9.930(2)	17.4268(16)
<i>b</i> [Å]	20.053(5)	18.4963(8)	17.734(3)	17.727(4)	17.4268(16)
<i>c</i> [Å]	12.521(3)	13.2675(5)	9.8466(15)	9.872(2)	25.094(5)
<i>α</i> [°]	90	90	90	90	90
<i>β</i> [°]	123.696(2)	90.819(4)	90.939(2)	91.173(2)	90
<i>γ</i> [°]	90	90	90	90	90
<i>V</i> [Å ³]	1531.2(7)	1774.57(14)	1709.5(5)	1737.4(6)	7620.9(18)
space group	<i>P21/c</i>	<i>P21/n</i>	<i>C2/c</i>	<i>C2/c</i>	<i>I4(1)/a</i>
<i>Z</i> value	4	4	4	4	4
ρ_{calc} [g cm ^{−3}]	1.672	2.128	2.391	2.690	2.784
$\mu(\text{MoK}\alpha)$ [mm ^{−1}]	1.956	29.273	4.893	12.416	6.557
<i>T</i> [K]	293(2)	293(2)	293(2)	293(2)	293(2)
<i>F</i> (000)	776	1064	1136	1264	5776
GOF	1.005	1.104	1.128	1.027	1.224
<i>R₁</i> / <i>wR₂</i> [<i>I</i> > 2 σ (<i>I</i>)]	0.0583/0.1155	0.0907/0.2577	0.0245/0.0605	0.0346/0.0834	0.0609/0.1464

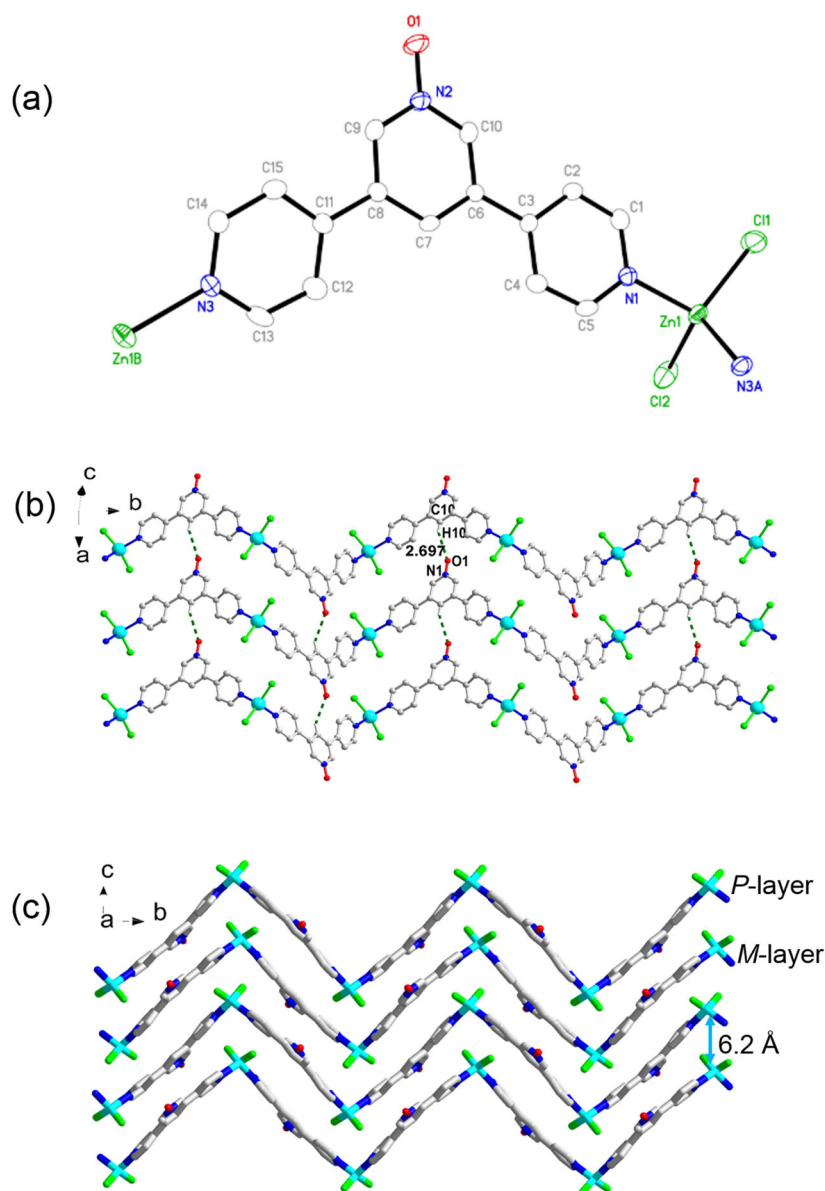


Figure 1. a) ORTEP drawing of the structure of **1**. Ellipsoids are given at the 50% probability level. b) Hydrogen-bonding-driven 2D net composed of 1D chains. c) Crystal packing of **1**.

the crystallographic *c* axis and the interchain zinc(II) distance is about 6.2 Å.

M^{II} CPs based on L2

The crystallization of L2 with CdI₂ and HgI₂ (metal-to-ligand ratio 1:1) in mixtures of THF/CH₃OH and CH₂Cl₂/CH₃OH at room temperature afforded **3** and **4** as colorless crystals, respectively. Single-crystal XRD reveals that complexes **3** (Cd(L2)₂) and **4** (Hg(L2)₂) are isostructural; they all feature 1D ripple-like chains (Table 1). Therefore, only the structure of **4** is described in detail herein.

Compound **4** crystallizes in the monoclinic space group C2/*c* (Figure 2a) and each mercury(II) node is located in a distorted tetrahedral {HgN₂I₂} coordination sphere, which is composed of

two pyridyl N-donors (*d*_{Hg–N} bond lengths are 2.406(6) Å) and two I[–] counterions. Similarly to **1** and **2**, the pyridine *N*-oxide group in **4** is also uncoordinated.

Figure 2b shows that L2 links HgI₂ units through terminal pyridyl N donors to create a one-handed 1D helix that extends along the crystallographic *c* axis. The *P* and *M* helices are further held together to provide double-stranded chains through interchain H⋯π interactions (Figure 2c). In the solid state, these double-stranded chains arrange along the crystallographic *a* axis, and no detectable interactions are found among them.

Catalytic properties

The Knoevenagel reaction, which is the condensation of active methylene compounds with aldehyde or ketone, is an impor-

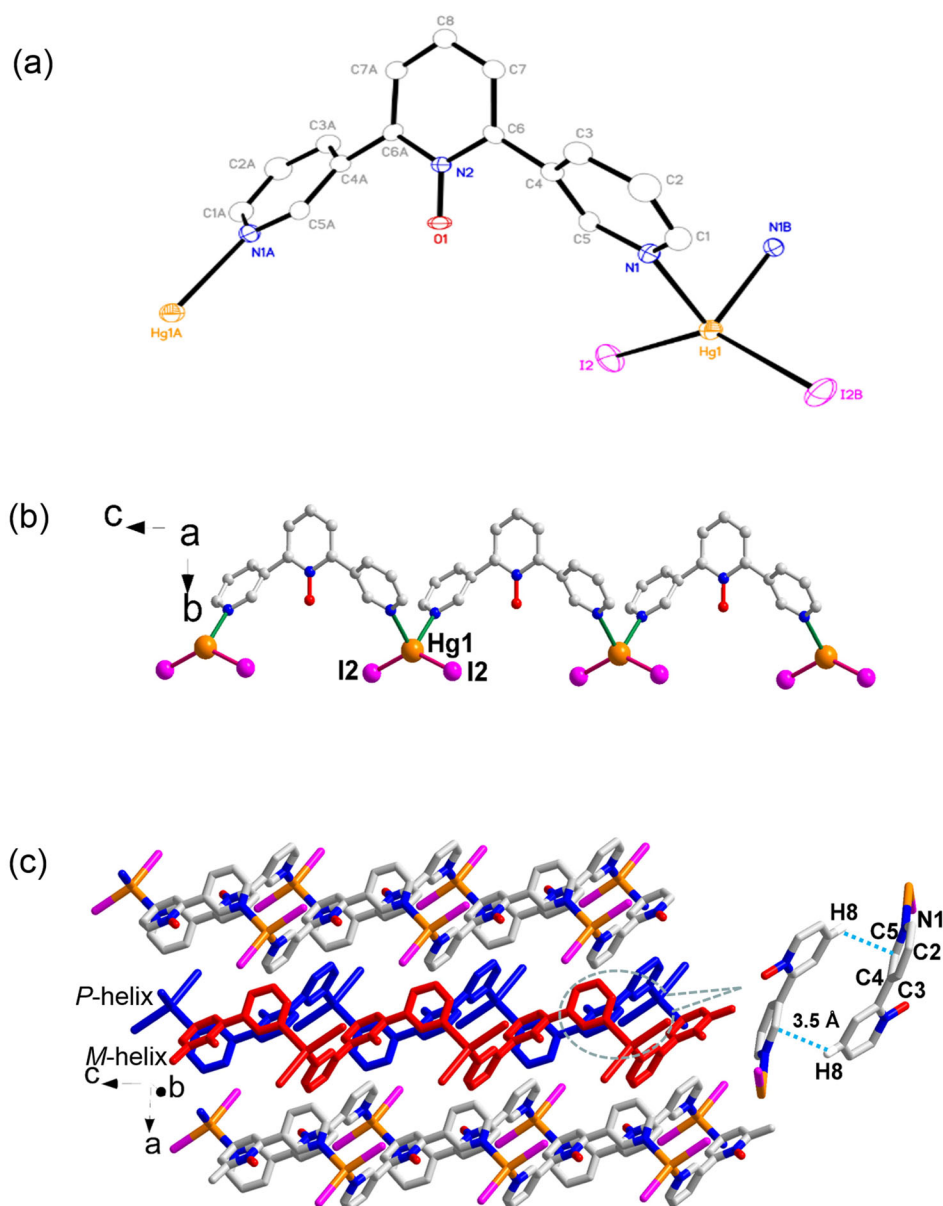


Figure 2. a) ORTEP drawing of the structure of **4**. Ellipsoids are given at the 50% probability level. b) Single 1D helical chain. c) Crystal packing of **4**.

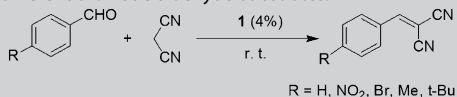
tant C–C coupling reaction and is widely used in the synthesis of fine chemicals. This type of condensation is generally catalyzed by Lewis bases or acids. As shown above, CPs **1–4** contain an open pyridyl *N*-oxide group and M^{II} nodes that could be considered as bifunctional catalysts. Such coexisting acid–base CPs would be more active than those of acid- or base-centered catalysts. Based on their structural features, compounds **1–4** are expected to show good catalytic behavior for Knoevenagel condensation under milder conditions.

On the other hand, aromatic *N*-oxides are potential pollutants of soils and aquatic environments because of their widespread use as antibiotics, pesticides, and other industrial chemical products.^[11] Therefore, the development of corresponding heterogeneous, eco-friendly, reusable, *N*-oxide-type catalysts for Knoevenagel condensation is a topic of great interest.^[12]

Consequently, the catalytic activity of compounds **1–4** as solid heterogeneous catalysts in the Knoevenagel condensation reaction of benzaldehydes with malononitrile was investigated.

Compound **1** was chosen to optimize the reaction conditions. In a typical reaction, condensation is performed under atmospheric pressure at room temperature. A mixture of benzaldehyde, malononitrile (1:1.2, molar ratio), and **1** (4 mol%, finely ground) was stirred at room temperature, and the reaction was monitored by GC. The GC–MS spectra (see the Supporting Information) indicated that the condensation reaction was finished in 6 h to afford 2-benzylidenemalononitrile as the expected product with excellent conversion (99.5%) and selectivity (99.2%; Table 2, entry 1). Notably, the condensation reaction described herein needed no additional organic solvents. Therefore, because this reaction is easy to manipulate and

Table 2. Catalytic data for the Knoevenagel condensation of malonitrile with different aromatic aldehyde substrates.



R = H, NO₂, Br, Me, t-Bu

Entry	R	Solvent	t [h]	Conv. [%] ^[c]	Selec. [%] ^[c]
1	-H	- ^[a]	6	99.5	99.2
2	-NO ₂	MeOH ^[b]	2	99.5	100
3	-Br	MeOH	2	99.5	100
4	-CH ₃	-	6	99	99.6
5	-tBu	-	6	97	97.1

[a] Solvent-free conditions. [b] MeOH was added to dissolve the substrates 4-methylbenzaldehyde and 4-*tert*-butylbenzaldehyde. [c] As determined by GC-MS analysis.

avoids the use of toxic and volatile solvents, it could be considered as a clean, catalytic organic synthesis approach. Compound **1** is stable in aqueous media over a wide pH range of 2–11 (see the Supporting Information), which makes it potentially a green catalyst to promote other organic reactions in aqueous solutions.

To explore the effect of substituents for this condensing reaction, different types of benzaldehydes were used as substrates under the reaction conditions. The results are summarized in Table 2. When 4-nitro- and 4-bromobenzaldehyde, with -NO₂ and -Br electron-withdrawing groups at the *para* positions are used, the conversions (99.5%, see the Supporting Information) of the condensing products are equivalent to that of benzaldehyde, but with the 100% selectivity. On the other hand, when electron-donating groups, namely, methyl and *tert*-butyl groups, were used as the substituents on benzaldehyde at the *para* position (4-methyl- and 4-*tert*-butylbenzaldehyde), slightly lower conversions (97–99%, see the Supporting Information) and selectivities (97.1–99.6%, see the Supporting Information) than those substrates containing electron-withdrawing groups were observed. Such an observation suggests that the electron-withdrawing substituents promote reactivity; this might be related to an increase in the electrophilicity of the substituted benzaldehydes. In addition, condensation reactions of benzaldehydes containing an electron-withdrawing group with malonitrile took only 2 h to reach 99.5% conversion (Table 2, entries 2 and 3), which strongly supported the above observation.

As shown above, compound **1** is nonporous. Thus, catalysis based on **1** should occur on the external surface. To prove this hypothesis, as-synthesized bulk crystals (average > 100 μm) of **1** were used instead of a finely ground sample (average < 20 μm; see the Supporting Information). The yield for the condensation of benzaldehyde and malonitrile was also up to 99.5%, but took a much longer time (10.5 h). This observation strongly indicates that catalysis by **1** exhibits surface catalytic behavior and is highly dependent on the catalyst particle size.

A control reaction was performed with benzaldehyde in the absence of **1**, at room temperature without solvent, and the

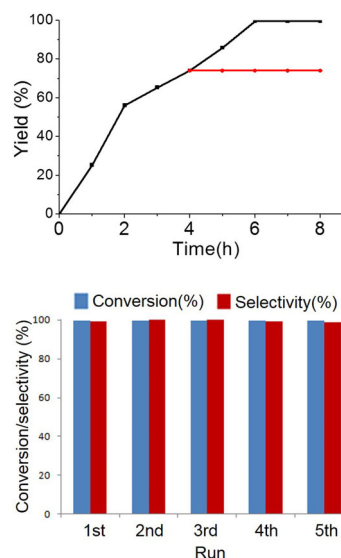


Figure 3. Above: Leaching test for catalytic condensation with compound **1**. Below: Results for the conversion and selectivity of the reaction between benzaldehyde and malonitrile catalyzed by **1** in five catalytic cycles.

yield of the condensation product was very low ($\approx 24\%$) after 6 h; this indicates that **1** is a highly active catalyst for the condensation of benzaldehyde and malonitrile under the reaction conditions described herein. To gain an insight into the heterogeneous nature of **2**, leaching tests were performed. As indicated in Figure 3, no further reaction took place without **1** after initiation of the reaction at 4 h (Figure 3).

Compound **1** can be reused as a heterogeneous catalyst. After each catalytic cycle, compound **1** could be easily recovered by centrifugation and filtration, and directly reused in the next run under the same reaction conditions. As indicated in Figure 3, after five consecutive catalytic runs, the conversion was still above 99% (see the Supporting Information), which indicated almost no degradation in the catalytic activity of **1** during the recycling process. In addition, compound **1** was demonstrated to be highly crystalline from analysis of the powder XRD patterns, even after five catalytic runs (Figure 4), which confirmed the reusability of **1** as a heterogeneous catalyst.

In addition, the catalytic properties of **2–4** were also explored under the same reaction conditions. For example, the treatment of benzaldehyde (1.0 mmol) with malonitrile (1.2 mmol) in the presence of **2–4** (4 mol%) at room temperature afforded the condensation products with very high conversions (99.5%, as determined by GC; see the Supporting Information), which were comparable to that of **1** (Table 3). Compared with the Zn^{II}-CPs **1** and **2**, the Knoevenagel reactions catalyzed by **3** and **4** with Cd^{II} centers required a longer reaction time (8 h). Different catalytic performances of **1/2** and **3/4** might be due to different metal centers and pyridyl *N*-oxide orientations resulting from the crystal-packing styles. The stronger Lewis acid zinc(II) center and more exposed *N*-oxide moieties in **1** and **2** would certainly facilitate this condensation reaction.^[13]

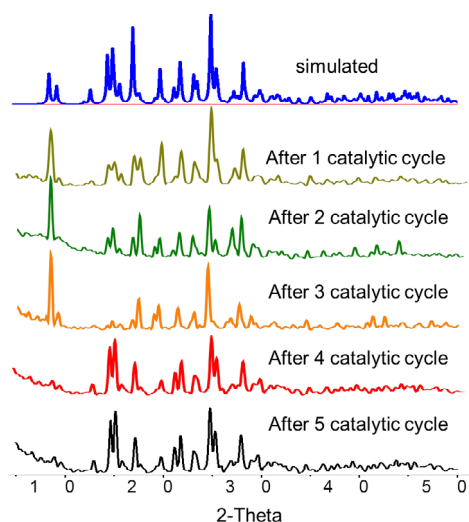


Figure 4. Simulated powder XRD pattern of **1** and those recorded after each catalytic cycle.

Entry	CP catalyst	<i>t</i> [h]	Conv. [%] ^[b]	Selec. [%] ^[b]
1	2	6	99.5	> 99
2	3	8	99.5	> 99
3	4	8	99.5	> 99

[a] Reaction conditions: benzaldehyde (1 mmol), malononitrile (1.2 mmol), catalyst (4% with respect to the amount of benzaldehyde), solvent-free conditions. [b] Yield determined by GC analysis.

To confirm the catalytic function of the open pyridyl *N*-oxide, we tried to prepare the CP without a free pyridyl *N*-oxide moiety. Through the combination of **L1** and CdI₂ in CH₂Cl₂/MeOH, compound **5** (Cd₆(L1)₄)₁₂ was generated. Single-crystal analysis indicated that **5** crystallized in the tetragonal space group *I4*(1)/*a* (Table 1). Different from **1** and **2**, ligand **L1** in **5** acts as a tridentate linker instead of a bidentate one to bind cadmium(II) nodes into a twofold interpenetrating 3D network with a two-nodal net (Schläfli symbol {4²;6}2{4⁴;6²;8²;10⁴7}; see the Supporting Information), in which all pyridyl *N*-oxides on **L1** coordinate to cadmium(II) centers and no open *N*-oxide sites remain (Figure 5). Indeed, when the condensation reaction of benzaldehyde and malononitrile was performed in the presence of **5** under the same reaction conditions, the reaction afforded much lower conversion (only ≈ 51% based on GC analysis), even after 12 h. We believe that this is only a metal-centered (Lewis acid) catalytic process.

In addition, a control reaction for the condensation of benzaldehyde with malononitrile was performed in the presence of 4,4'-bispyridyl-*N,N'*-dioxide as a catalyst under the same reaction conditions, the yield for the expected condensing product was 99.5% (5 h); this yield was the same as those obtained for reactions catalyzed by **1–4** (see the Supporting Information). This result further demonstrated that the open pyridyl *N*-

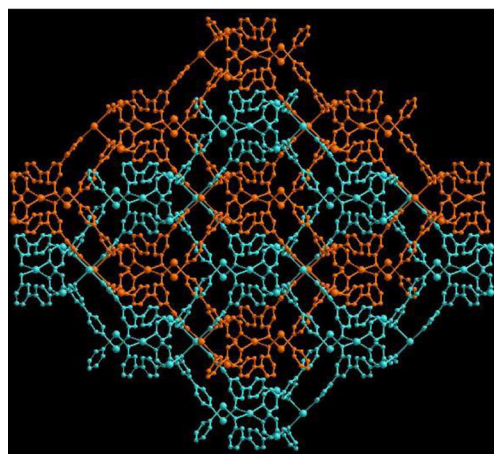
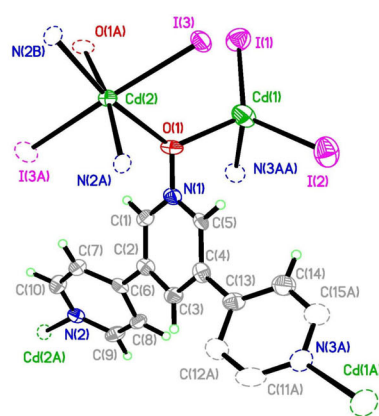


Figure 5. Above: ORTEP drawing of the structure of **5**. Ellipsoids are given at the 50% probability level. The *N*-oxide coordinates to the Cd^{II} center with Cd–O bond lengths of 2.319(8) and 2.510(8) Å. Below: b) Twofold interpenetrating network in **5**.

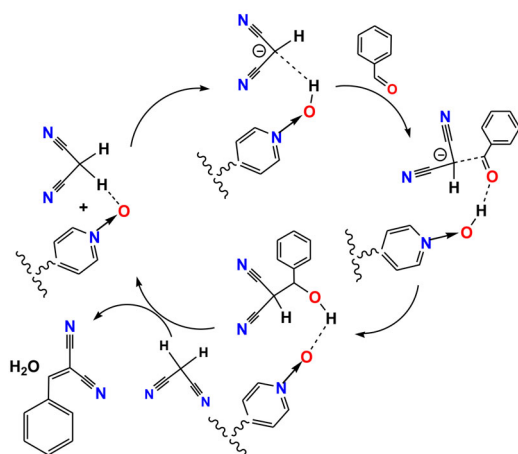
oxide was the dominating active catalytic site for Knoevenagel condensation.

Based on the above observation, the condensation between benzaldehyde and malononitrile might follow the reaction pathway shown in Scheme 3.

To date, a series of CPs as catalysts for the Knoevenagel condensation of benzaldehyde and malononitrile have been reported (Table 4). The conversions in our system based on **1–4** are usually higher than those reported for other zinc(II) and cadmium(II) CPs. In addition, most of reactions are performed under solvent-assistant conditions and require a longer time or higher temperature. Therefore, CPs **1–4** are good solid catalysts with the advantages of being easy to prepare, energy saving, and resulting in clean synthesis. More importantly, the ligand-centered CP catalysts described herein might provide a useful approach to access new types of CP catalysts.

Conclusion

We successfully synthesized four M^{II} CPs (M = Zn, Cd, Hg) based on pyridyl *N*-oxide bridging ligands. All four CPs featured a 1D chain motif and contained open pyridyl *N*-oxide sites. More importantly, these CPs could be used as highly active heteroge-



Scheme 3. The proposed mechanism for the Knoevenagel condensation of benzaldehyde and malononitrile in **1**.

Table 4. Comparison of the catalytic activity of typical CPs in the Knoevenagel reaction of benzaldehyde and malononitrile.

Entry	CP catalyst	Conditions	Conv. [%]	Ref.
1	Zn ₂ dobdc	toluene/70 °C/24 h	77	[14]
2	Zn ₂ (tpt) ₂ (2-atp) ₂	ethanol/60 °C/2 h	99	[15]
3	[Ni ₄ (μ ₆ -MTB) ₂ (μ ₂ -H ₂ O) ₄ (H ₂ O) ₄]-10 DMF·11 H ₂ O	<i>p</i> -xylene/130 °C/6 h	78	[16]
4	[Tb(BTATB)(DMF)(H ₂ O) ₂]-DMF·2 H ₂ O	CH ₃ CN/60 °C/24 h	99	[17]
5	[Cd(4-btapa) ₂ (NO ₃) ₂]-6 H ₂ O·2 MDF	benzene/RT/12 h	98	[18]
6	Pb(cpna) ₂ ·2 MDF·6 H ₂ O	CH ₃ CN/RT/24 h	quant	[19]
7	[ZnL(H ₂ O) ₂] <i>n</i> DMF	THF/40 °C/1.5 h	98	[20]
8	ZIF-8	toluene/RT/3 h	100	[21]
9	TMU-5	solvent-free/RT/4 h	96	[22]
10	(H ₃ O) ₂ [Cd ₃ (2,7-CDC) ₄]-3 DMF·4 H ₂ O	DMF/RT/3 h	quant	[23]
11	ZIF-9	toluene/RT/6 h	99	[24]
12	TS-1	xylene/130 °C/6 h	96	[25]
13	Cu-BTC	xylene/130 °C/1 h	quant	[25]
14	Fe-BTC	xylene/130 °C/3 h	quant	[25]
15	1-4	solvent-free/RT/6–8 h	99.5	this study

dobdc = 2,5-dioxidoterephthalate; tpt = 2,4,6-tris(4-pyridyl)-1,3,5-triazine; 2-atp = 2-aminoterephthalate; MTB = methanetetra benzoate; BTATB = 4,4'4''-benzene-1,3,5-triyl-tris(azanediyl)tribenzoate; 4-btapa = 1,3,5-benzene tricarboxylic acid tris[*N*-(4-pyridyl)amide]; cpna = *N*-(4-carboxyphenyl)isonicotinamide 1-oxide; L = 5-acetamidoisophthalic acid; 2,7-CDC = 9*H*-carbazole-2,7-dicarboxylic acid; BTC = benzene-1,3,5-tricarboxylate; quant = quantitative.

neous catalysts to promote the Knoevenagel reaction under mild conditions. The catalytic functions of free pyridyl *N*-oxides were demonstrated. We believe that this new ligand-design approach will be very useful for the synthesis of more ligand-centered CP catalysts. Compared with metal-centered CP counterparts, the ligand-centered CP catalysts are beneficial supplements to the CP catalyst family. More heterogeneous CP catalysts of this type are currently under investigation in our laboratory.

Experimental Section

Materials and methods

HgI₂, ZnCl₂, CdI₂, and ZnI₂ (Acros) were used as obtained without further purification. IR samples were prepared as KBr pellets, and spectra were obtained in the $\tilde{\nu}$ = 400–4000 cm⁻¹ range by using a PerkinElmer 1600 FTIR spectrometer. Elemental analyses were performed on a PerkinElmer model 2400 analyzer. ¹H NMR data were collected by using an AM-300 spectrometer. Chemical shifts are reported in δ relative to tetramethylsilane (TMS). Powder XRD patterns were obtained on a D8 ADVANCE powder X-ray diffractometer with Cu_{K α} radiation (λ = 1.5405 Å). GC-MS analysis data were recorded on a J&K S011525-300 gas chromatograph (Agilent 6890GC-5973MS). Separation data were obtained by using an Agilent 1260 Infinity HPLC system equipped with an Agilent C18 reverse-phase column (150 × 4.6 mm, 5 μ m).

Ligand synthesis

Synthesis of 3,5-dibromopyridine *N*-oxide: 3,5-Dibromopyridine (3.2 g, 13.5 mmol) was dissolved in THF (50 mL), mCPBA (4.6 g, 26.5 mmol) was added, and the mixture was heated at reflux for 48 h. A saturated aqueous solution of Na₂CO₃ (25–30 mL) was added until the resulting mixture became basic. The aqueous layer was extracted with CH₂Cl₂ (2 × 50 mL) and the combined organic layers were dried over Na₂SO₄. The crude product was purified by column chromatography on silica gel with CH₂Cl₂ as the eluent to afford 3,5-dibromopyridine *N*-oxide as a white crystalline solid (1.5 g, 59.3%). ¹H NMR (300 MHz, DMSO, 25 °C, TMS): δ = 8.60 (s, 2H; -C₅H₃NBr₂), 7.97 ppm (s, 1H; -C₅H₃NBr₂).

Synthesis of 2,6-dibromopyridine *N*-oxide: 2,6-Dibromopyridine (4.7 g, 20 mmol) was dissolved in CH₂Cl₂ (50 mL) and the UHP adduct (4.0 g, 42 mmol) was added. The mixture was cooled to 0 °C and then TFAA was slowly added. A saturated aqueous solution of Na₂S₂O₃ (25–30 mL) and a solution of Na₂CO₃ were added until the resulting mixture became basic. The aqueous layer was extracted with CH₂Cl₂ (2 × 50 mL) and the combined organic layers were dried over Na₂SO₄. The crude product was purified by column chromatography on silica gel with CH₂Cl₂ as the eluent to afford 2,6-dibromopyridine *N*-oxide as a white crystalline solid (3.3 g, 58.9%). ¹H NMR (300 MHz, [D₆]DMSO, 25 °C, TMS): δ = 7.95 (d, 2H; -C₅H₃NOBr), 7.12 ppm (t, 1H; -C₅H₃NOBr).

Synthesis of L1: A solution of 3,5-dibromopyridine *N*-oxide (1.73 g, 10.0 mmol), pyridine-4-boronic acid (2.95 g, 24.0 mmol), K₂CO₃ (17.25 g, 125.0 mmol), and [Pd(PPh₃)₄] (1.16 g, 1.0 mmol) in EtOH/H₂O was heated at reflux for 40 h under N₂ (Scheme 1). After removal of solvent under vacuum, the residue was purified by column chromatography to afford **L1** (72%). IR (KBr pellet): $\tilde{\nu}$ = 3048 (m), 2469 (w), 1603 (s), 1552 (m), 1502 (w), 1462 (w), 1406 (s), 1348 (w), 1217 (m), 1174 (m), 1069 (m), 1013 (m), 943 (w), 821 (s), 679 (w), 625 (w), 557 cm⁻¹ (w); ¹H NMR (300 MHz, [D₆]DMSO, 25 °C, TMS): δ = 8.84 (s, 2H; -C₅H₃NO-), 8.73–8.72 (d, 4H; -C₆H₄N-), 8.18 (s, 1H; -C₆H₃NO-), 7.95–7.94 ppm (d, 4H; -C₆H₄N-); elemental analysis calcd (%) for C₁₅H₁₁N₃O: C 72.58, H 4.44, N 16.87; found: C 72.01, H 4.85, N 16.24.

Synthesis of L2: A solution of 2,6-dibromopyridine *N*-oxide (1.73 g, 10.0 mmol), pyridine-3-boronic acid (2.95 g, 24.0 mmol), K₂CO₃

(17.25 g, 125.0 mmol), and [Pd(PPh₃)₄] (1.16 g, 1.0 mmol) in EtOH/H₂O was heated at reflux for 40 h under N₂ (Scheme 1). After removal of solvent under vacuum, the residue was purified by column chromatography to afford **L2** (75%). IR (KBr pellet): $\tilde{\nu}$ = 3046 (s), 1603 (s), 1552 (m), 1503 (w), 1463 (w), 1408 (s), 1343 (w), 1225 (m), 1174 (m), 1069 (w), 1011 (m), 943 (w), 822 (s), 679 (w), 625 (w), 557 cm⁻¹ (w); ¹H NMR (300 MHz, [D₆]DMSO, 25 °C, TMS): δ = 8.84 (s, 2H; -C₅H₃NO-), 8.73–8.72 (d, 4H; -C₆H₄N-), 8.18 (s, 1H; -C₆H₃NO-), 7.95–7.94 ppm (d, 4H; -C₆H₄N-); elemental analysis calcd (%) for C₁₅H₁₁N₃O: C 72.58, H 4.44, N 16.87; found: C 72.11, H 4.96, N 16.45.

Synthesis of M^{II} CPs

Synthesis of Zn(L1)Cl₂ (1): A solution of ZnCl₂ (2.7 mg, 0.02 mmol) in CH₃OH (5 mL) was carefully layered on a solution of **L1** (5 mg, 0.02 mmol) in CH₂Cl₂ (5 mL). The solution was left for 1 week at room temperature, and colorless crystals of **1** were obtained (53% (based on **L1**)). IR (KBr pellet): $\tilde{\nu}$ = 3099 (w), 1616 (s), 1552 (m), 1514 (w), 1402 (m), 1342 (m), 1199 (s), 1075 (m), 1028 (m), 949 (w), 823 (s), 691 (w), 643 (m), 604 (w), 499 cm⁻¹ (m); elemental analysis calcd (%) for C₁₅H₁₁ZnCl₂N₃O: C 46.70, H 2.85, N 10.90; found: C 47.14, H 2.48, N 10.55.

Synthesis of Zn(L1)₂ (2): A solution of ZnI₂ (7 mg, 0.02 mmol) in CH₃OH (5 mL) was carefully layered on a solution of **L1** (5 mg, 0.02 mmol) in CH₂Cl₂ (5 mL). The solution was left for 1 week at room temperature, and colorless crystals of **2** were obtained (50% (based on **L1**)). IR (KBr pellet): $\tilde{\nu}$ = 3069 (s), 1602 (s), 1550 (s), 1503 (w), 1401 (s), 1344 (s), 1068 (m), 1010 (m), 946 (w), 819 (s), 674 (m), 626 (m), 552 cm⁻¹ (w); elemental analysis calcd (%) for C₁₅H₁₁HgI₂N₃O: C 25.60, H 1.56, N 5.97; found: C 25.88, H 1.48, N 6.21.

Synthesis of Cd(L2)₂ (3): A solution of CdI₂ (7.33 mg, 0.02 mmol) in CH₃OH (5 mL) was carefully layered on a solution of **L2** (5 mg, 0.02 mmol) in THF (5 mL). The solution was left for 1 week at room temperature, and yellow crystals of **3** were obtained (47% (based on **L2**)). IR (KBr pellet): $\tilde{\nu}$ = 3070 (s), 1601 (s), 1551 (m), 1501 (w), 1465 (w), 1412 (s), 1344 (w), 1324 (w), 1174 (m), 1014 (m), 942 (m), 824 (m), 782 (m), 692 (m), 628 cm⁻¹ (m); elemental analysis calcd (%) for C₁₅H₁₁CdI₂N₃O: C 29.25, H 1.79, N 6.82; found: C 29.67, H 1.94, N 6.51.

Synthesis of Hg(L2)₂ (4): A solution of HgI₂ (10 mg, 0.02 mmol) in CH₃OH (5 mL) was carefully layered on a solution of **L2** (5 mg, 0.02 mmol) in CH₂Cl₂ (5 mL). The solution was left for 1 week at room temperature, and colorless crystals of **4** were obtained (57% (based on **L2**)). IR (KBr pellet): $\tilde{\nu}$ = 3046 (w), 1602 (s), 1551 (s), 1503 (w), 1462 (w), 1408 (s), 1345 (m), 1220 (w), 1173 (s), 1069 (w), 1012 (m), 941 (m), 824 (s), 680 (w), 627 cm⁻¹ (w); elemental analysis calcd (%) for C₁₅H₁₁HgI₂N₃O: C 25.60, H 1.56, N 5.97; found: C 25.94, H 1.32, N 6.22.

Synthesis of Cd₆(L1)₄I₁₂ (5): A solution of CdI₂ (7.33 mg, 0.02 mmol) in CH₃OH (5 mL) was carefully layered on a solution of **L1** (5 mg, 0.02 mmol) in CH₂Cl₂ (5 mL). The solution was left for 1 week at room temperature, and colorless crystals of **5** were obtained (44% (based on **L2**)). IR (KBr pellet): $\tilde{\nu}$ = 3043 (s), 1604 (s), 1550 (s), 1502 (w), 1462 (w), 1405 (s), 1344 (m), 1220 (w), 1205 (s), 1171 (s), 1069 (w), 1010 (m), 938 (m), 826 (s), 679 (w), 628 (w), 556 cm⁻¹ (w); elemental analysis calcd (%) for C₆₀H₄₄Cd₆I₁₂N₁₂O₄: C 33.05, H 2.02, N 7.71; found: C 33.27, H 1.88, N 7.46.

Typical catalytic experiment

A mixture of benzaldehyde (1.0 mmol, 0.1 mL), and malononitrile (1.2 mmol, 0.079 g) was stirred at ambient temperature for 5 min., and then the CP catalyst (4%) was added. The mixture was stirred for 6–8 h at room temperature (monitored by GC) and the conversions and products were determined by GC-MS. The catalyst was recovered by filtration, washed with methanol, and then directly reused in the next run under the same reaction conditions.

Single-crystal structure determination

Suitable single crystals of **1–5** were selected and mounted in air onto thin glass fibers. X-ray intensity data were measured at 298(2) K on a Bruker SMART APEX CCD-based diffractometer (Mo_{K α} radiation, λ = 0.71073 Å). The raw frame data for **1–5** were integrated into SHELX-format reflection files and corrected for Lorentz and polarization effects by using SAINT.^[26] Corrections for incident and diffracted beam adsorption effects were applied by using SADABS.^[10] None of the crystals showed evidence of crystal decay during data collection. All structures were solved by a combination of direct methods and difference Fourier syntheses and structural analysis refined against F^2 by the full-matrix least-squares technique. Crystal data, data collection parameters, and refinement statistics for **1–5** are listed in Table 1. Relevant interatomic bond lengths and angles for **1–5** are given in Tables S1–S5 in the Supporting Information. CCDC 1443513–1443517 contain the supplementary crystallographic data for this paper. These data can be obtained free of charge from The Cambridge Crystallographic Data Centre.

Acknowledgements

We are grateful for financial support from the NSFC (grant nos. 21475078 and 21271120), the 973 Program (grant nos. 2012CB821705 and 2013CB933800), and the Taishan Scholar's Construction Project.

Keywords: coordination polymers • heterogeneous catalysis • Knoevenagel condensation • pyridyl *N*-oxides • transition metals

- [1] a) J. R. Li, R. J. Kuppler, H. C. Zhou, *Chem. Soc. Rev.* **2009**, *38*, 1477; b) L. J. Murray, M. Dinca, J. R. Long, *Chem. Soc. Rev.* **2009**, *38*, 1294; c) G. Férey, *Chem. Soc. Rev.* **2008**, *37*, 191–214; d) M. P. Suh, H. J. Park, T. K. Prasad, D.-W. Lim, *Chem. Rev.* **2012**, *112*, 782; e) R. B. Getman, Y.-S. Bae, C. E. Wilmer, R. Q. Snurr, *Chem. Rev.* **2012**, *112*, 703.
- [2] a) M. D. Allendorf, C. A. Bauer, R. K. Bhakta, R. J. Houk, *Chem. Soc. Rev.* **2009**, *38*, 1330; b) Y. J. Cui, Y. F. Yue, G. D. Qian, B. L. Chen, *Chem. Rev.* **2012**, *112*, 1126.
- [3] a) M. Vallet-Regí, F. Balas, D. Arcos, *Angew. Chem. Int. Ed.* **2007**, *46*, 7548; *Angew. Chem.* **2007**, *119*, 7692; b) G. Férey, C. Serre, C. Mellot-Draznieks, F. Millange, S. Surblé, J. Dutour, I. Margiolaki, *Angew. Chem.* **2004**, *116*, 6456; c) Q. He, J. Shi, *J. Mater. Chem.* **2011**, *21*, 5845; d) P. Horcajada, T. Chalati, *Nat. Mater.* **2010**, *9*, 172.
- [4] a) M. Yoon, R. Srirambalaji, K. Kim, *Chem. Rev.* **2012**, *112*, 1196; b) L. Ma, C. Abney, W. Lin, *Chem. Soc. Rev.* **2009**, *38*, 1248; c) J. Y. Lee, O. K. Farha, J. Roberts, K. A. Scheidt, S. B. T. Nguyen, J. T. Hupp, *Chem. Soc. Rev.* **2009**, *38*, 1450; d) U. Czaja, N. Trukhan, U. Müller, *Chem. Soc. Rev.* **2009**, *38*, 1284; e) C. Wang, D. Liu, W. Lin, *J. Am. Chem. Soc.* **2013**, *135*, 13222; f) J. Liu, L. Chen, H. Cui, J. Zhang, L. Zhang, C.-Y. Su, *Chem. Soc. Rev.* **2014**, *43*, 6011; g) M. Zhao, S. Ou, C.-D. Wu, *Acc. Chem. Res.* **2014**, *47*, 1199; h) A. Dhakshinamoorthy, A. M. Asiri, H. Garcia, *Chem. Soc. Rev.*

- 2015, 44, 1922–1947; i) Q.-L. Zhu, X. Qiang, *Chem. Soc. Rev.* **2014**, 43, 5468.
- [5] a) K. Wang, D. Feng, T.-F. Liu, J. Su, S. Yuan, Y.-P. Chen, M. Bosch, X. Zou, H.-C. Zhou, *J. Am. Chem. Soc.* **2014**, 136, 13983–13986; b) L. Ma, C. D. Wu, M. M. Wanderley, W. Lin, *Angew. Chem. Int. Ed.* **2010**, 49, 8244–8248; *Angew. Chem.* **2010**, 122, 8420–8424; c) A. M. Shultz, O. K. Farha, D. Adhikari, A. A. Sarjeant, J. T. Hupp, S. T. Nguyen, *Inorg. Chem.* **2011**, 50, 3174.
- [6] a) S. Aguado, J. Canivet, D. Farrusseng, *J. Mater. Chem.* **2011**, 21, 7582; b) M. Banerjee, S. Das, M. Yoon, H. J. Choi, M. H. Hyun, S. M. Park, G. Seo, K. Kim, *J. Am. Chem. Soc.* **2009**, 131, 7524; c) D. J. Lun, G. I. N. Waterhouse, S. G. Telfer, *J. Am. Chem. Soc.* **2011**, 133, 5806.
- [7] a) J.-P. Ma, S.-Q. Wang, C.-W. Zhao, Y. Yu, Y.-B. Dong, *Chem. Mater.* **2015**, 27, 3805; b) Y.-A. Li, C.-W. Zhao, N.-X. Zhu, Q.-K. Liu, G.-J. Chen, J.-B. Liu, X.-D. Zhao, J.-P. Ma, S. Zhang, Y.-B. Dong, *Chem. Commun.* **2015**, 51, 17672; c) Q.-K. Liu, J.-P. Ma, Y.-B. Dong, *J. Am. Chem. Soc.* **2010**, 132, 7005; d) P. Wang, J.-P. Ma, Y.-B. Dong, R.-Q. Huang, *J. Am. Chem. Soc.* **2007**, 129, 10620; e) J.-C. Wang, F.-W. Ding, J.-P. Ma, Q.-K. Liu, J.-Y. Cheng, Y.-B. Dong, *Inorg. Chem.* **2015**, 54, 10865.
- [8] a) H.-Y. Wang, J.-Y. Cheng, J.-P. Ma, Y.-B. Dong, R.-Q. Huang, *Inorg. Chem.* **2010**, 49, 2416; b) J.-Y. Cheng, P. Wang, J.-P. Ma, Q.-K. Liu, Y.-B. Dong, *Chem. Commun.* **2014**, 50, 13672.
- [9] a) A. V. Malkov, P. Kocovsky, *Eur. J. Org. Chem.* **2007**, 29–36; b) S. E. Denmark, G. L. Beutner, *Angew. Chem. Int. Ed.* **2008**, 47, 1560; *Angew. Chem.* **2008**, 120, 1584; c) M. Nakajima, M. Saito, M. Shiro, S.-i. Hashimoto, *J. Am. Chem. Soc.* **1998**, 120, 6419; d) T. Shimada, A. Kina, S. Ikeda, T. Hayashi, *Org. Lett.* **2002**, 4, 2799; e) J. Chen, B. Captain, N. Takenaka, *Org. Lett.* **2011**, 13, 1654; f) I. Kim, S. W. Roh, D. G. Lee, C. Lee, *Org. Lett.* **2014**, 16, 2482; g) W. Wang, M. Kumar, G. B. Hammond, B. Xu, *Org. Lett.* **2014**, 16, 636.
- [10] a) H. He, D. Collins, F. Dai, X. Zhao, G. Zhang, H. Ma, D. Sun, *Cryst. Growth Des.* **2010**, 10, 895; b) K. O. Kongshaug, H. Fjellvåg, *Inorg. Chem.* **2006**, 45, 2424.
- [11] Y. Chen, H. Dong, H. Zhang, *Environ. Sci. Technol.*, **2016**, 50, 249.
- [12] a) P. Valvekens, D. Jonckheere, T. De Baerdemaeker, A. V. Kubarev, M. Vandichel, K. Hemelsoet, M. Waroquier, V. Van Speybroeck, E. Smolders, D. Depla, M. B. J. Roeffaers, D. De Vos, *Chem. Sci.* **2014**, 5, 4517; b) M. Zhao, K. Deng, L. He, Y. Liu, G. Li, H. Zhao, Z. Tang, *J. Am. Chem. Soc.* **2014**, 136, 1738; c) P. V. Dau, S. M. Cohen, *Inorg. Chem.* **2015**, 54, 3134; d) P. Serra-Crespo, E. V. Ramos-Fernandez, J. Gascon, F. Kapteijn, *Chem. Mater.* **2011**, 23, 2565.
- [13] N. Niklas, A. Zahlb, R. Alsfasser, *Dalton Trans.* **2007**, 154.
- [14] P. Valvekens, M. Vandichel, M. Waroquier, V. Van Speybroeck, D. De Vos, *J. Catal.* **2014**, 317, 1.
- [15] Y. Tan, Z. Fu, J. Zhang, *Inorg. Chem. Commun.* **2011**, 14, 1966.
- [16] M. Almáši, V. Zelenák, M. Opanasenko, J. Čejka, *Dalton Trans.* **2014**, 43, 3730.
- [17] N. Wei, M. Y. Zhang, X. N. Zhang, G. M. Li, X. D. Zhang, Z. B. Han, *Cryst. Growth Des.* **2014**, 14, 3002.
- [18] S. Hasegawa, S. Horike, R. Matsuda, S. Furukawa, K. Mochizuki, Y. Kinoshita, S. Kitagawa, *J. Am. Chem. Soc.* **2007**, 129, 2607.
- [19] X. M. Lin, T. T. Li, L. F. Chen, L. Zhang, C.-Y. Su, *Dalton Trans.* **2012**, 41, 10422.
- [20] A. Karmakar, G. M. D. M. Rúbio, M. F. C. G. da Silva, S. Hazra, A. J. L. Pombeiro, *Cryst. Growth Des.* **2015**, 15, 4185.
- [21] U. P. N. Tran, K. K. A. Le, N. T. S. Phan, *ACS Catal.* **2011**, 1, 120.
- [22] M. Y. Masoomi, S. Beheshti, A. Morsali, *Cryst. Growth Des.* **2015**, 15, 2533.
- [23] X.-C. Yi, M.-X. Huang, Y. Qi, E.-Q. Gao, *Dalton Trans.* **2014**, 43, 3691.
- [24] L. T. L. Nguyen, K. K. A. Le, H. X. Truong, N. T. S. Phan, *Catal. Sci. Technol.* **2012**, 2, 521.
- [25] M. Opanasenko, A. Dhakshinamoorthy, M. Shamzhy, P. Nachtigall, M. Horacek, H. Garcia, J. Čejka, *Catal. Sci. Technol.* **2013**, 3, 500.
- [26] SAINT, Bruker Analytical X-ray Systems, Inc., Madison, WI, **1998**.

Manuscript received: January 8, 2016

Revised: March 3, 2016

Accepted Article published: March 11, 2016

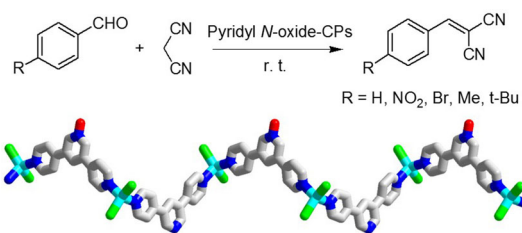
Final Article published: ■ ■ ■, 0000

FULL PAPERS

J.-Y. Cheng, F.-W. Ding, P. Wang,
C.-W. Zhao, Y.-B. Dong*



Synthesis, Structure, and Ligand-Centered Catalytic Properties of M^{II} Coordination Polymers ($M = Zn^{II}$, Cd^{II} , Hg^{II}) with Open Pyridyl *N*-Oxide Sites



Metal infiltration: A series of one-dimensional M^{II} coordination polymers (CPs) with open pyridyl *N*-oxide sites are reported. These CPs can be used as

highly active heterogeneous catalysts for Knoevenagel condensation under ambient conditions (see scheme).